

# Enhancing Performance of Hybrid Natural Fiber Reinforced Polymer: Insights into Processing, Characterization and Machining

Vivek Sheel Rajput<sup>1</sup>, Mohinder Pal Garg<sup>2</sup>, Sarbjit Singh<sup>3,\*</sup>

## Abstract

Natural fibre reinforced polymer composites (N-FRP) have gained popularity in recent years as an alternative to regular polymer composites, owing to growing environmental concerns. Natural fibers are becoming increasingly popular due to their outstanding properties such as flexibility, strength, compatibility with living creatures, and impact resistance. A notable application of natural fibers is in the medical industry, with the goal of producing cost-effective, sustainable, and long-lasting products. Combining different fibers in the matrix can improve a material's mechanical characteristics in a hybrid method where one type of fibre can compensate for the deficiencies of another. Since the volume of fibers greatly affect the mechanical characteristics of hybrid composite materials, our present study is to investigate the effect of volume fraction of jute and sisal fibers on tensile strength of hybrid composite followed by machining using rotary electrochemical discharge-based machining (R-ECDM) process. The holes are fabricated at different electrolyte concentration and rotation of the tool. The hole overcut (HOC), Circularity error (CE) and surface roughness (SR) of the machined hole is analyzed to study the impact of input process parameter. ECDM applies the principle of thermal heating and chemical etching to remove the material and effectively applied for non-conductive brittle materials. The article's originality lies in the combined characterization study of hybridized N-FRP and its machining using R-ECDM. The tensile strength of composites improves as the volume of fibers increases due to the influence of individual fibre strengths. The proposed machining method is analyzed for machinability study of the N-FRP hybrid composites. The rotational effect improves the HOC, CE and surface roughness of the machined hole due to enhanced circulation of the electrolyte. The input parameters significantly affect the input parameters since all response parameters increases with the increase of electrolyte concentration and at higher level of tool rotation.

**Keywords:** Natural fibers, hybrid composite, volume fraction, ECDM, sparks, surface roughness

### \*Author for Correspondence

Sarbjit Singh

<sup>1</sup>Assistant Professor, Department of Mechanical Engineering, Punjab Engineering College, Chandigarh, Punjab, India

<sup>2</sup>Associate Professor, Department of Mechanical Engineering, Punjab Engineering College, Chandigarh, Punjab, India

<sup>3</sup>Professor, Department of Mechanical Engineering, Punjab Engineering College, Chandigarh, Punjab, India

Received Date: June 09, 2024

Accepted Date: October 10, 2024

Published Date: January 23, 2025

**Citation:** Vivek Sheel Rajput, Mohinder Pal Garg, Sarbjit Singh. Enhancing Performance of Hybrid Natural Fiber Reinforced Polymer: Insights into Processing, Characterization and Machining. Journal of Polymer & Composites. 2025; 13(Special Issue 2): S139–S153p.

## INTRODUCTION

Composite materials are made up of two or more components that have diverse properties at the microscopic and macroscopic levels. Straw bricks were employed in architecture as early as 10,000 B.C., while laminated composites from the papyrus plant were utilized as writing material in 4,000 B.C. The Mangolas created contemporary composite bows out of flexible materials including cattle tendons, wood, and silk around 1,200 B.C [1]. These materials surpass traditional materials in terms of fatigue life, energy dissipation, corrosion resistance, and cost-effectiveness. Polymer composites comprising high-strength fibers such as glass, carbon etc. are becoming increasingly used in

industries such as aerospace, automotive, construction and biomedical [2]. They outperform conventional materials in terms of stiffness, strength, and weight [3]. However, the manufacturing of these synthetic polymer matrix composites requires a large amount of energy and raises environmental issues after their lifecycle. Synthetic polymers contribute to global environmental challenges such as non-biodegradable trash and the depletion of petroleum resources [4].

To address these concerns and promote sustainability, there is a rising emphasis on developing polymers based natural fibers. Plant-derived biopolymers such as starch, rubber, and poly-lactic acid are blended with natural fibers such as hemp, ramie, sisal, bagasse, banana, jute, flax, aloe vera, and bamboo. According to literature studies, the composition of pectin, lignin, hemicellulose, and cellulose in these natural fibers varies depending on the plant part. This shift to N-FRP composites helps to a more sustainable and environmentally responsible future.

Natural fibre composites derived from plants, such as bamboo, jute, cotton, coir, hemp, and bagasse, are eco-friendly, lightweight, durable, renewable, and biodegradable. They are commonly used in situations needing better performance to strengthen both thermosetting and thermoplastic matrices [5]. Natural fibre advancements, like as genetic engineering, provide sustainable materials, opening up potential for global sustainability. Because of their low cost and environmental benefits, these composites are used in building, packaging, vehicle and railway coach interiors, and storage devices. While their low density and inexpensive cost are advantages, resolving their greater moisture absorption requires chemical treatments [6]. The classification of the fibers is given in Figure 1. Jute, a bast fibre derived from the plants *Corchorus capsularis* is grown largely for its affordability and value as a natural fibre, ranking second only to cotton [7]. Sisal produces strong fibers with full biodegradability, high tenacity, outstanding tensile strength, toughness, abrasion resistance, resistance to acids and alkalis, corrosion resistance, and seawater resilience [8]. As a result, sisal is an excellent material for the manufacture of green composites [9]. Despite this, natural fibre composites are being evaluated as viable replacements for high-cost glass fibre in several applications. NFRP composites are finding widespread use in a variety of engineering sectors. Many automotive businesses, including Opel, Mercedes, Proton, Daimler Chrysler, BMW, Ford, Cambridge industry (an auto industry in the United States), Volkswagen, and Audi Group, have placed a high value on natural fibre reinforced polymer composites in various automotive applications. Aside from the automotive business, natural fibre composites have found applications in sports, the building and construction industry, aerospace, and others, including as panels, window frames, decking, and bicycle frames [10].

Several studies [11,12]. have been conducted to investigate the appropriateness and competitiveness of natural fibers in polymeric matrices. Others concentrated on improving fiber/polymer compatibility by modifying surface properties and production techniques [13,14]. Several studies compared the application stability of various natural fibre composites. Lopez et al. [15]. observed that reinforcing flax fibre in flax/PLA composites using biodegradable polymers such as Polylactic acid (PLA) resulted in better mechanical characteristics than carbon/epoxy composites. This shows that natural fibre composites have the potential to replace synthetic fibers in terms of mechanical performance.

Keck et al [16]. investigated flax fiber-reinforced composites and discovered distinct crack pathways under static and fatigue loading. Extensive numerical simulations were used to examine stress intensity factor evolution and provide a technique for calculating geometry correction factors, revealing that higher fibre volume fractions result in higher young's moduli and tensile strengths. Okubo et al [17]. focused on the development of a new composite material by combining bamboo fibre and polypropylene. Their study sought to comprehensively investigate and comprehend the mechanical behaviour of these composite materials, providing light on their potential uses and attributes. Jiang et al [18]. investigated the mechanical properties of composites made of poly(3-hydroxybutyrate-co-3-hydroxyvalerate) and bamboo fibre. Nino Serah Baby et al. [19]. used agricultural waste to create a polymer matrix supplemented with sisal fibre for commercial composite manufacture. The study found

that lignocellulosic fibers have greater impact strength despite having conventional flexural and tensile properties. The mechanical properties of natural hybrid composites made from vinyl ester, sisal, glass, steel fibre, and Prosopis Juli flora were investigated. Fibre kinds, cultivation, growing duration, retting or extracting procedure, isolation, and processing processes all have an impact on natural fibre qualities [20]. Numerous research has been conducted to evaluate the effect of fibre types and processing methods on natural fibre composite tensile strength, Young's modulus, density, and elongation at break [10]. Finally, the research and implementation of hybrid N-FRP have opened new novel possibilities for improving the durability and longevity of diverse structures, particularly in industries that require robust and resilient materials. The use of natural fibers like sisal and jute demonstrates the transdisciplinary nature of materials science and engineering. As research advances, the potential for analyzing N-FRP composites and machining them with R-ECDM remains an intriguing prospect.

In the meanwhile, ECDM method has shown useful for cutting non-conductive materials such as glass and quartz [21]. To remove or drill materials, this technique employs heat melting and chemical dissolving principles. Figure 2 depicts the ECDM process, in which two electrodes - a tool electrode and an auxiliary electrode - are immersed in an electrolyte, which is typically an alkali substance such as aqueous NaOH or KOH. A potential difference across the electrodes is created by applying a pulsed or continuous direct current source, which initiates electrolysis and the formation of hydrogen and oxygen gas bubbles at the cathode and anode, respectively. These bubbles coalesce due to ohmic heating and electrochemical processes, generating an insulating layer or hydrogen film near the tool electrode. This film, known as tool blanketing, temporarily stops current flow while establishing a strong electric field that surround it.

The breakup of the gas film at a critical voltage ( $V_c$ ) enhances the emergence of electrical sparks across the tool and electrolyte. Notably, the electrolyte content influences viscosity, with larger concentrations resulting in smoother machined surfaces due to increased chemical activity [22].

Kurafuji & Suda [23]. gave introduction of ECDM for micro-drilling holes in glass laid the groundwork for following advances in precision machining. They emphasized the highest attainable drilling depths for glass machining. Basak and Ghosh expanded upon this by presenting on a theoretical model to determine critical voltage and current values required for sparking in ECDM [24,25]. This model was useful in understanding and forecasting the efficient and accurate machining features of glass materials. Zheng et al. [26] extended the use of ECDM to milling operations, demonstrating its potential to generate complex three-dimensional microstructures on glass. Malik & Manna [27]. investigated the machinability of a non-conductive E-glass fibre composite with a NaOH electrolyte and discovered a proportionate rise in MRR with applied voltage. The significance of surfactant-enhanced electrolyte was emphasized by Rajput et al. [28], who noted that a higher concentration promoted chemical activity as well as electrical conductivity, improving the geometrical aspects of the machined surfaces. In comparison to ECDM without tool rotation, tool rotation also improves the MRR, geometric properties, and dimensional accuracy of the micro-holes [29]. The uniform distribution of sparks is achieved by preventing the occurrence of sparks at a single place through tool electrode rotation. Tool electrode rotation serves in preventing the sparks just at a single spot and generates uniform sparks dispersion [30]. It stops stray corrosion from happening, which could lead to improved hole circularity. Nonetheless, an extensive amount of experimental research has been done to enhance the ECDM process's machining performance [31-34]. An investigation on how tool rotation affects hole characteristics during the ECDM micro-hole production process is critically presented [35]. The findings demonstrate that while tool rotation results in micro-holes with improved circularity, it also results in a degraded hole shape. Bhargav et al. [36] utilized a rotary aided ECDM methodology to examine the machining properties of carbon fiber-reinforced polymer (CFRP) composites. The research addressed constraints such inadequate electrolyte availability, demonstrating the capability of R-ECDM to surmount obstacles related to conventional CFRP machining using ECDM. Rajput et al [37,38]. also fabricated and investigated the machining of polymer composites using ECDM process.

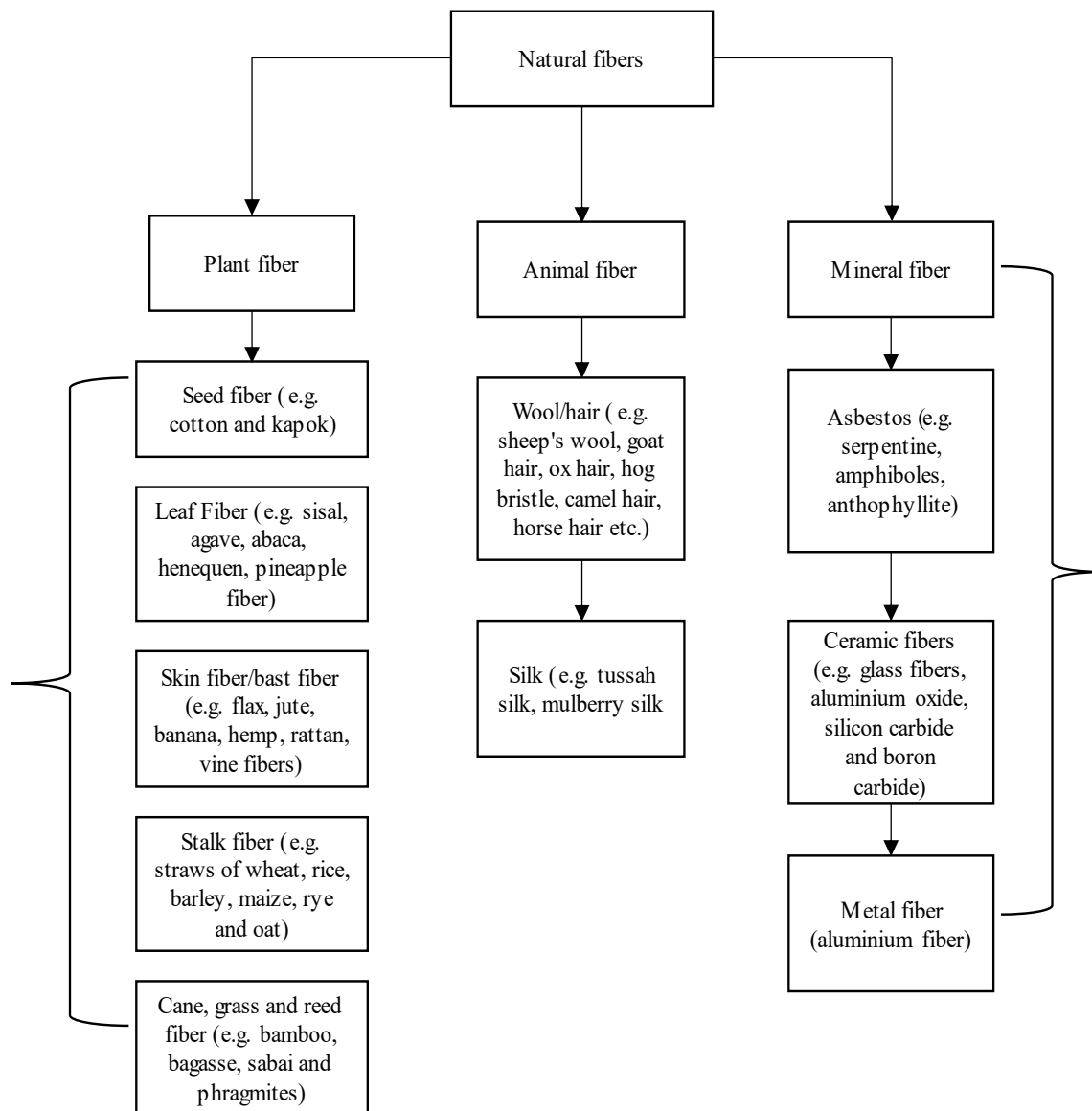


**Figure 1.** Classification of the natural fibers (Mohammed et al., 2015).

In addition, researchers have explored the complex interplay in the ECDM process between discrete response variables and input process parameters [39,40]. Their combined knowledge lays the groundwork for comprehending how modifications of these variables can best utilize ECDM's multi-response characteristics, thus improving the system's overall effectiveness. Essentially, the development of ECDM is a result of an ongoing process of improving and investigating its precision machining capabilities, with an emphasis on enhancing productivity and output quality.

### Problem Formulation

Literature reveals that many experimental studies have been performed to investigate the polymers composites as well as its machining potential using non-conventional machining methods. So far, the machining of the hybrid N-FRP composite made of Sisal and Jute using R-ECDM process has never been reported. The present study analyses the effect of jute and sisal fiber's volume fraction on tensile strength followed by its machining using R-ECDM. The surface roughness of the machined hole on a hybrid composite is also studied for various electrolyte concentration as well as for various tool rotations.

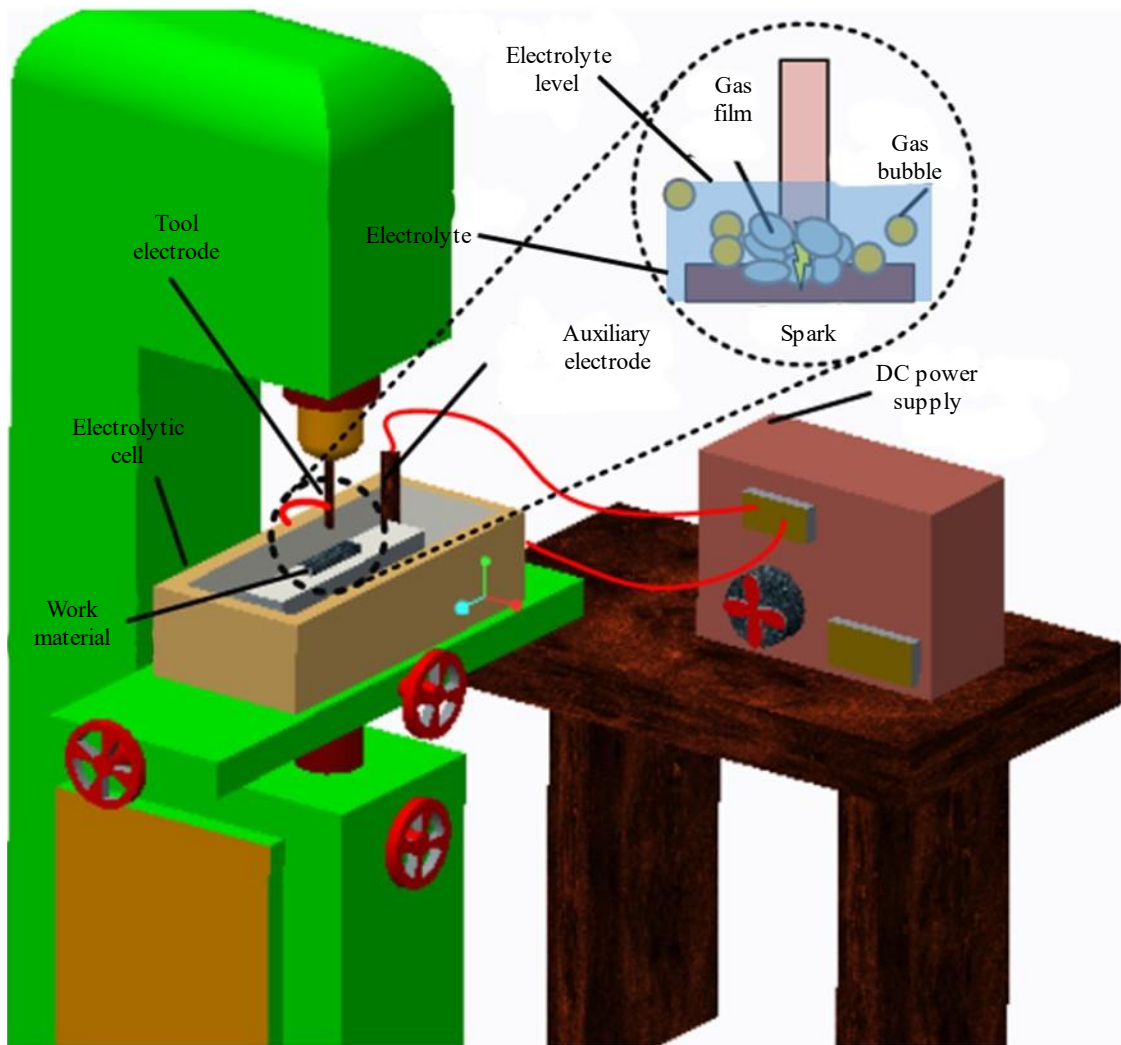


**Figure 2.** Principle schematic diagram of ECDM Process [22].

### RESEARCH METHOD AND EXPERIMENTAL SETUP

The experimentation of the present work is carried out in two phases i.e., (i) Fabrication and tensile strength analysis of the hybrid N-FRP and (ii) Machinability study through hole fabrication using R-ECDM (Figure 3). Phase I: The hand-layup technique was utilized to create a hybrid N-FRP composites consisting of uni-directional Sisal and Jute fibers. Using the hand-layup method, four layers of fibers were integrated with epoxy resin (matrix) throughout the fabrication process. The composite was put under 150 kg of weight at room temperature for 36 hours. The sample was then taken out of the die and weighed to get the final composite weight. Using a micrometer, the final sample's thickness was determined. To assess the tensile strength, five N-FRP composite specimens (named as P1, P2, P3, P4, and P5) are constructed. The specimens have been chosen based on ASTM specifications for size and shape. Table 1 lists the specifics, designation, fibre type, and fiber volume fraction of the hybrid N-FRP composite specimens. Figure 4 shows the microscopy images of the fabricated N-FRP hybrid composite. The Jute and Sisal fibers are clearly visible in the top view of the composite as seen in Figure 4. The Phase II: the experiments are carried out on an established gravity feed experimental setup integrated to a vertical milling machine in order to investigate the impact of tool rotation on machining parameters by comparing them with those obtained in the absence of tool rotation. The tool electrode is cylindrical in shape and composed of stainless steel with a diameter of 1 mm. The input variables and additional machining conditions used in this investigation are shown in Table 2. The hole fabrication time of 2 minutes is utilized in all the cases. A stereo microscope is used to analyze the machined holes

from the top view side. Tool rotation (rpm) and electrolyte concentration (wt%) are the input factors taken into account in this study, and surface roughness is chosen as a response characteristic. The High to Low Temperature Tribometer is an advanced roughness measuring device used to assess the surface roughness (SR) of the holes created on N-FRP during the R-ECDM process. This instrument makes it feasible to precisely measure and investigate the surface characteristics of the holes made using various tool rotation and electrolyte concentration.

**RESULTS AND DISCUSSIONS**

**Tensile Strength Assessment**

An experimental investigation of the tensile strength is performed to assess the effect of volume fraction of the fibers in hybrid N-FRP composites. Figure 5 shows the tensile strength obtained after tensile test of the hybrid and single fibers reinforced composites. In polymer composites, fibers serve as a reinforcing component that greatly increases the material's tensile strength. The enhanced resistance against cracking and fracture under tension is ascribed to the fibers' ability to more efficiently distribute and withstand tensile loads inside the composite structure, hence averting stress concentration.

**Table 1.** Includes information on the fibre’s volume fraction, and their types in the fabricated composite specimens.

S N.	Titled	Fiber type	Volume fraction (%)	Objective
1.	P <sub>1</sub>	Jute Fibers	20	To study the effect of fiber volume fraction on Tensile strength
2.	P <sub>2</sub>	Sisal Fibers	20	
3.	P <sub>3</sub>	Hybrid (Jute + Sisal)	20	
4.	P <sub>4</sub>	Hybrid (Jute + Sisal)	30	
5.	P <sub>5</sub>	Hybrid (Jute + Sisal)	40	

**Table 2.** Includes information on the machining conditions during hole fabrication using R-ECDM.

Input variable	Range	Input variable	Range
Tool material	SS ( $\Phi = 1000 \mu\text{m}$ )	Applied Voltage	40 V
Electrolyte	NaOH	Electrolyte level	1 mm
Tool rotation	355, 560 & 900 rpm	Electrolyte concentration	15-30 wt.%

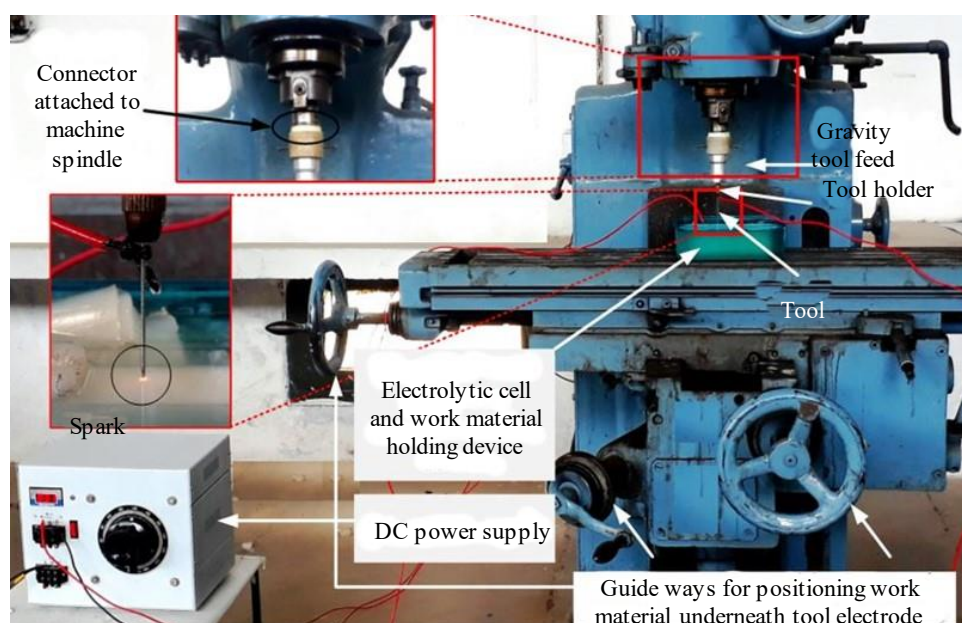


**Figure 3.** Designed gravity feed assisted R-ECDM configuration (Rajput et al., (2021).

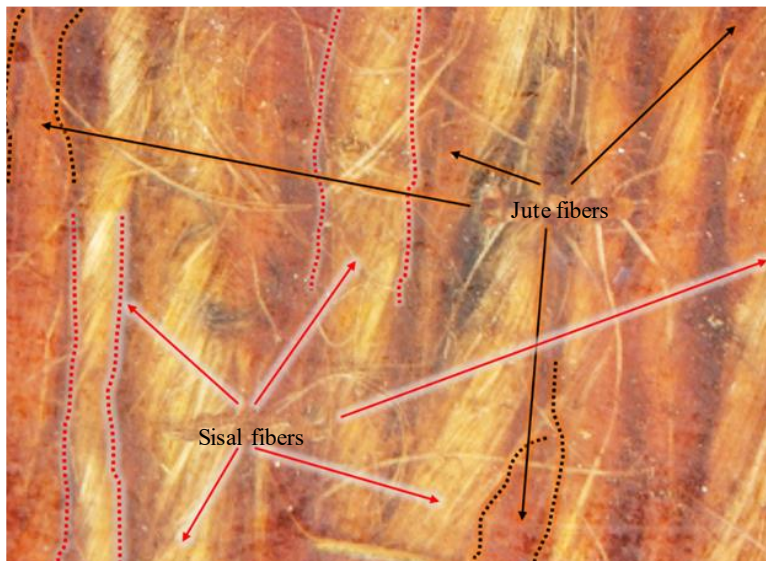


**Figure 4.** Prepared N-FRP hybrid composite.

It is observed that at the same fibre loading, Jute fiber reinforced composites outperform Sisal fiber reinforced composites in terms of tensile strength (P1 & P2). The results are supported by the previous reported in the comparative study of Jute/Epoxy and Sisal/Epoxy composites [41].

Further it is observed that with the hybridization of the N-FRP composites, the tensile strength is increased further at similar volume fraction of fibers due to the synergistic effect of both the fibers in composites as shown in Figure 5. An increase of 44.9% is noticed with the hybridization of the composites with a Jute/Sisal fiber (P3) when compared to sisal fiber reinforced composites (P2). It is concluded that when sisal and jute fibers hybridize, the distinct properties of each fibre are combined to create a composite material that has a synergistic reinforcement of tensile strength. This leads to better mechanical qualities, increased resistance to fracture and cracking under tension, which further makes the hybrid composite more resilient.

Figure 6 shows the microscopy cross-sectional images of the hybrid damaged composite after tensile test at 20% volume fraction. With the increase in fiber volume fraction of the fibers, the tensile strength is increased further due to increase in resistance given by the fibers during loading (P4 & P5).

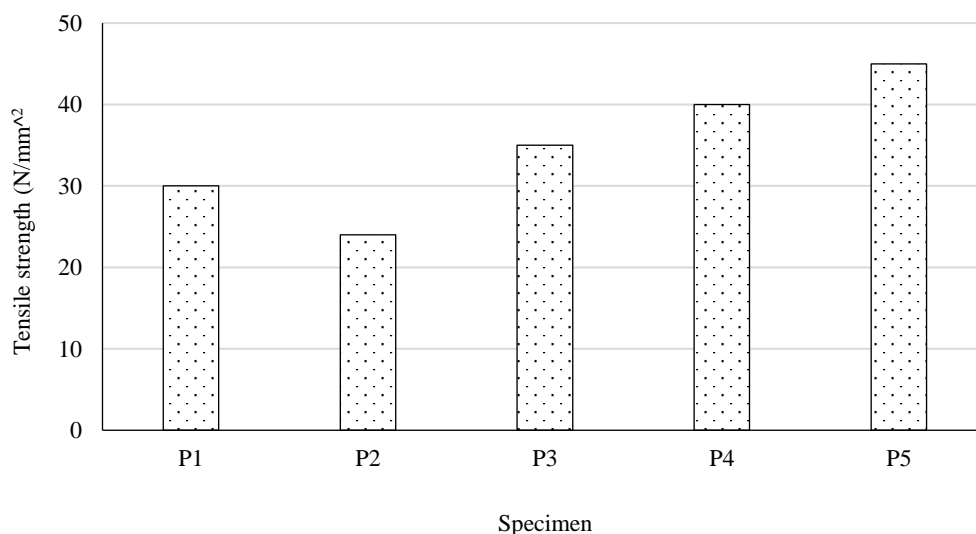


**Figure 5.** Tensile strength comparison of different specimens.

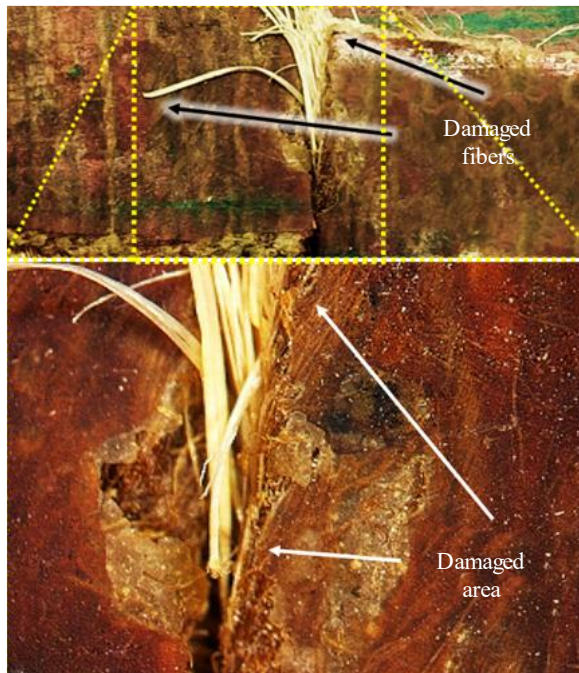


**Figure 6.** Damaged hybrid composite after tensile test at 20% volume fraction of jute & sial fibers.

### Effect of Volume Fraction on Tensile Strength

Figure 5 presents that with the increase in fiber volume fraction, there is an increase in tensile strength due to enhancement in the individual fiber percentage that increase the load bearing capacity of the hybrid N-FRP composites. The increase in volume fraction increases the load bearing capacity of each of the fiber which further enhances the tensile strength when hybridized. Figure 7 shows the microscopy cross-sectional images of the damaged composite after tensile test at two different volume fractions of Jute & Sisal fibers. The torn out of the fibers are clearly visible in the images after being pulled out during the tensile test. The volume fraction of fibers in a composite material has a synergistic effect on its tensile strength because it is a crucial parameter in defining its mechanical performance. Because the fibers in the composite are reinforcing, any increase in the fibre volume percentage also results in the improvement of tensile strength (Figure 5 & 7). A notable increase of 28.42% is computed with the increase of 20% in Jute/Sisal fiber volume fraction. An increase in fiber volume fraction leads to better load-bearing capacity results from the fibers' ability to more evenly distribute and share applied tensile stresses, which lessens the chance of early failure and stress concentrations.

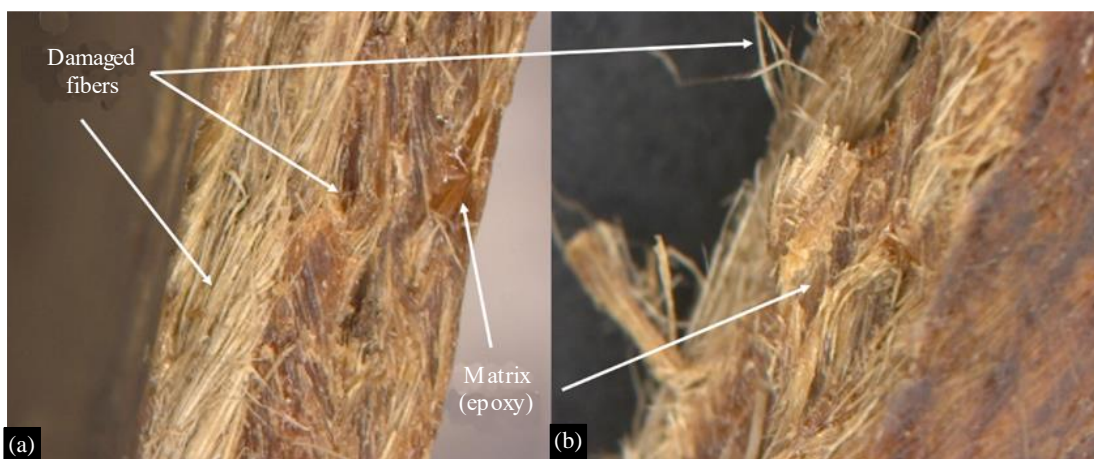


**Figure 7.** Damaged hybrid composite after tensile test at two different volume fraction of Jute & Sial fibers (a) 30% (b) 40 wt.%.

### Micro-Hole Fabrication Using R-ECDM

The holes are successfully machined on hybrid N-FRP composites using R-ECDM process at various level of electrolyte concentration and tool rotation as visible in Figure 8. The condition of the holes in the N-FRP is analyzed to study the surface roughness and its geometrical characteristics in terms of hole overcut (HOC) and circularity error (CE).

The HOC and CE are computed using below expressions given in Equations 1 & 2. HOC is described as the difference of the tool electrode's ( $D_t$ ) diameter and the calculated diameter of the hole entry of the drilled holes on N-FRP ( $D_{ent}$ ) (Figure 9 (a)). The CE is described as the out of roundness error and illustrate hole geometrical accuracies. It is calculated as the difference of the hole's highest value of diameter and smallest value of the diameter as displayed in Figure 9 (b).

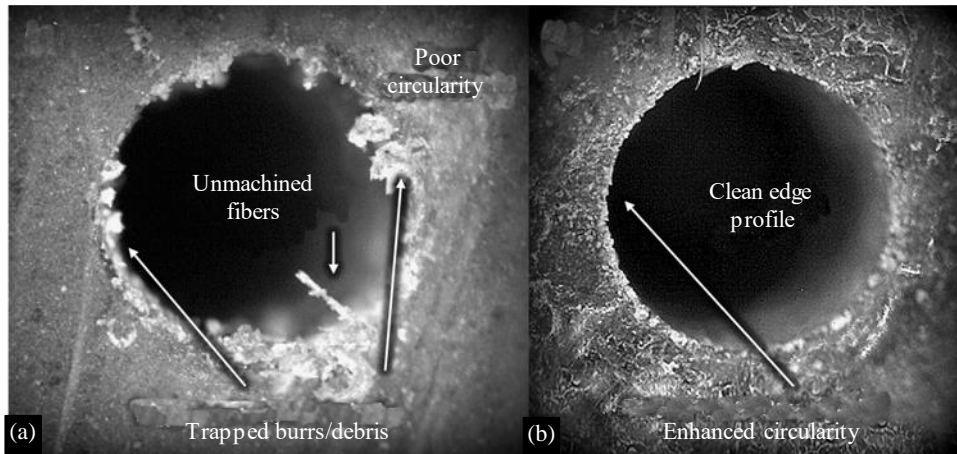
$$HOC = D_t - D_{ent} \quad \text{Eq. (1)}$$

$$CE = R_{high} - R_{small} \quad \text{Eq. (2)}$$

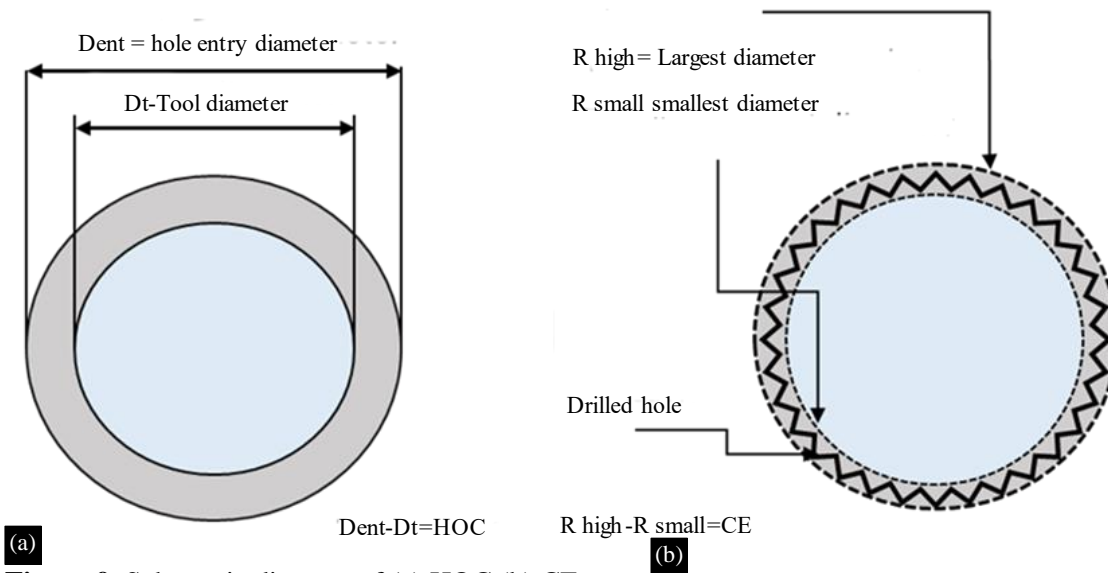
It is observed that the hole geometry is greatly improved by tool rotation as it prevents sparks from originating at one location. When tool rotation is used, the hole geometry improves significantly as compared to holes that are produced without rotation (Figure 8). Figure 10 shows the plot of HOC and CE at different electrolyte concentration. It is observed that both HOC and CE both improves with the application of the tool rotation. An improvement of 36.3 % and 29.8 % in HOC and CE is computed with the application of tool rotational effect in ECDM compared to conventional ECDM process. The primary cause of this improved geometry is the rotating effect's improved electrolyte replenishment below the tool electrode or in the drilling zone. As a result, the spark dispersion becomes more uniform, which enhances the thermal heating impact in the drilling zone. Additionally, the tool's rotating action helps to better remove sludge from the machining zone, which helps to keep fresh electrolyte in this area.

It is noticed that fibers or material remain unmachined and debris is entrapped at the hole edges when drilled using ECDM process (Figure 8(a)) while compared to hole geometry when drilled using R-ECDM process (Figure 8 (b)). A better circularity of hole is observed with R-ECDM process with increased electrolyte concentration, but the quality of the drilled hole deteriorates, resulting in an increase in HOC. When the concentration is increased from 20 wt.% to 25 wt.%, the HOC increases 13.6 %. (Figure 10 (a)). The reason for this is that thermal energy provided by the sparks in the ECDM process is proportional to the concentration of OH ions, which increases with the electrolyte concentration. Thus, with the increasing levels of electrolyte concentration, sparks occur more often from the sides of the tool electrode. It leads to the increase in HOC. The HOC improves initially as the tool rotational speed increases up to the first level from 355 rpm to 560 rpm. However, it gradually decreases as the tool rotation increases from 560 to 990 rpm. Rotation has a positive influence on HOC because it improves electrolyte availability and distributes heat energy evenly over the drilling area. HOC improves by 19.2 % with the first level increase in tool rotation and then increases further by 17 % with the next level increase of tool rotation. At higher level, the gas film becomes more unstable owing to centrifugal forces, resulting in electrolyte splashing. Consequently, the rate of improvement in HOC decreases. A similar trend is observed in the results of CE (Figure 10).

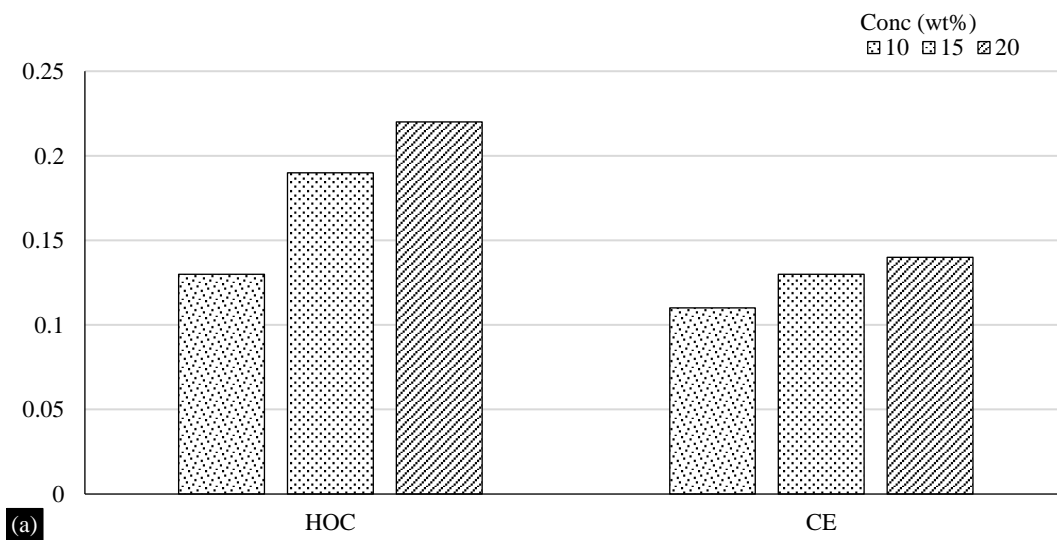
When tool rotation is used, the surface roughness of the hole is significantly reduced compared to surface roughness obtained without the application of tool rotation. Figure 11 shows the graphs of the surface roughness obtained using tribometer. An improvement of 39.8 % is noticed in surface roughness with the application of rotational effect to ECDM when compared to ECDM (Figure 11(a) & (b)). This reduction is due to the tool's ability to prevent side and stray sparking. It demonstrates the constant material removal at the hole edges, resulting in better circularity or geometry and surface roughness. The entrapment of debris or unmachined material at the hole edge also leads to poor surface roughness.



**Figure 8.** Microscopy images of the drilled holes on hybrid N-FRP using (a) conventional ECDM process (b) rotary ECDM process.



**Figure 9.** Schematic diagram of (a) HOC (b) CE.



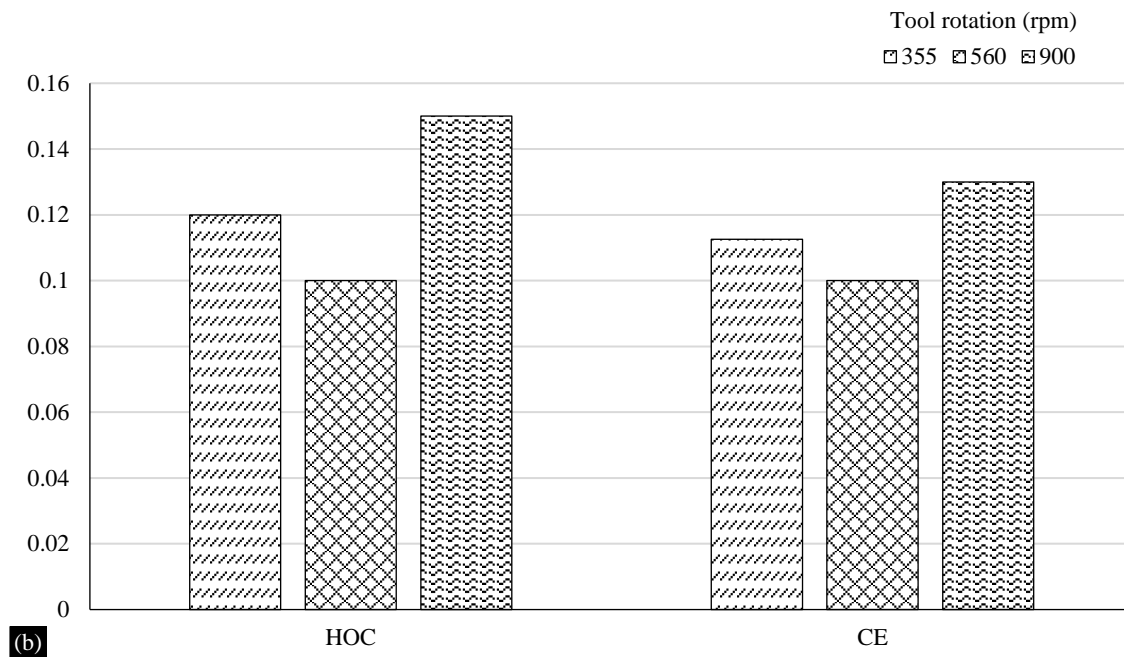


**Figure 10.** Schematic diagram of (a) HOC (b) CE.

Furthermore, it is noted that surface roughness values increase with the increase in both the tool rotation and electrolyte concentration (Figure 12). An increase of 15.8 % and 33% in surface roughness is noticed with the increase in electrolyte concentration from 15 wt.% to 20 wt.% (Figure 11 (b) & (c) and increase in tool rotation 355 rpm to 900 rpm (Figure 11 (b) & (d)) respectively. This rise is due to increased spark intensity and consistencies with increased frequency from the sides of the tools, which contributes to an increase in surface roughness.

Additionally, an increase in the electrolyte concentration leads to an improvement in the rate of bubble production, which in turn facilitates the rapid formation of the gas film. As a result, high spark frequencies are therefore obtained, strengthening the thermal energy transmission. An increase in electrolyte conductivity with a rise in electrolyte concentration accelerates the sparking rate [24,25]. Hence, at greater levels of input variables, a large number of thermal cracks and debris production are seen which further deteriorate the surface finish and leads to high roughness at the edges.

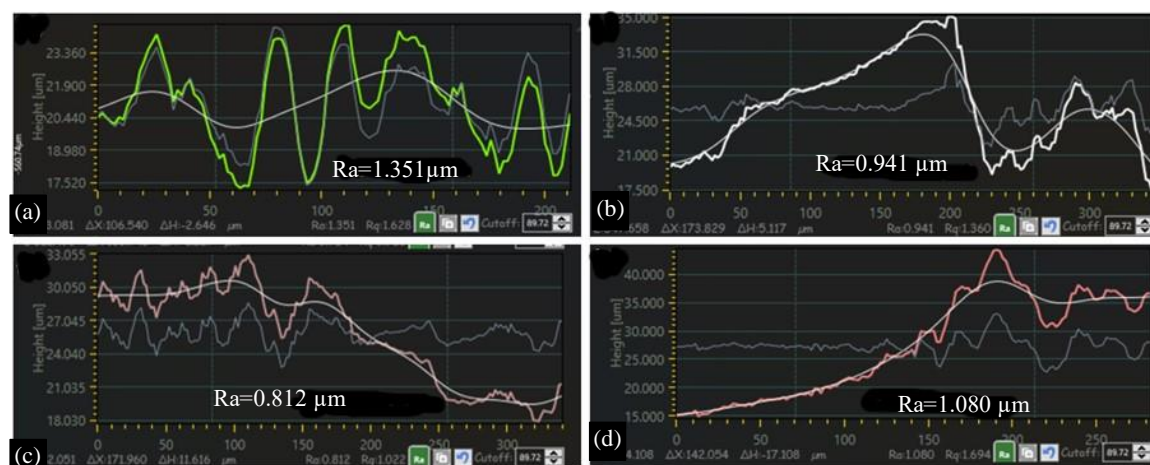


**Figure 11.** Surface roughness graphs at different input parameters (a) ECDM at 15 wt.% (b) R-ECDM, 15 wt.% & 355 rpm (c) R-ECDM at 20 wt.% & 355 rpm (d) R-ECDM at 15 wt.% & 900 rpm.

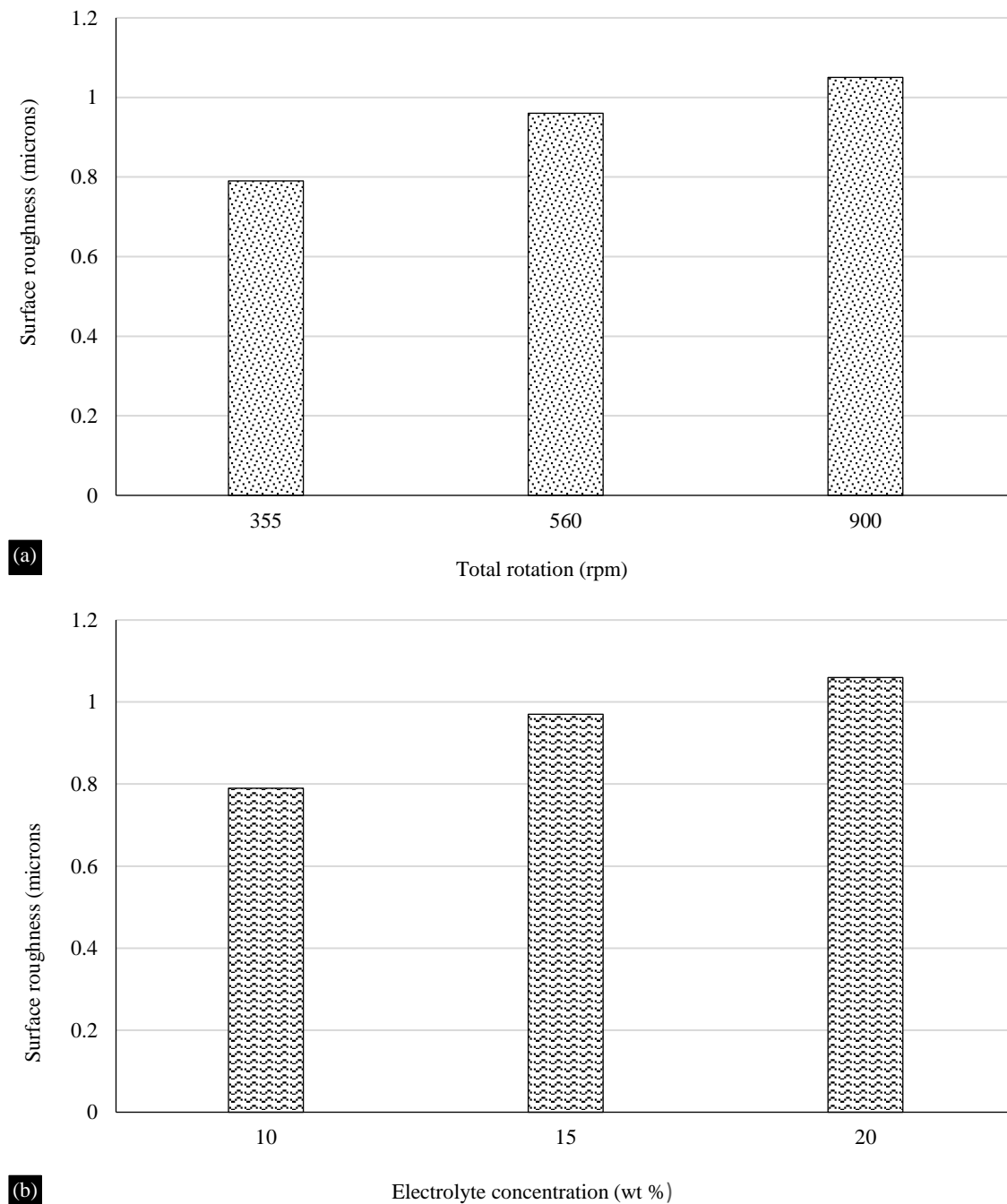


**Figure 12.** Surface roughness comparison of hybrid specimens at different electrolyte concentration and tool rotation.

## CONCLUSIONS

The present study investigates the effect of volume fraction of hybrid natural fibers (Jute/Sisal) on tensile strength of the composites followed by the machining investigation of the fabricated composites using R-ECDM. The effect of electrolyte concentration and tool rotational speed on surface roughness is also studied. The main conclusions of the study are:

- By effectively dispersing and restraining loads, natural fibers in polymer composites greatly increase tensile strength and avoid stress concentration.
- For the same fibre volume fraction, composites reinforced with jute fibers have a greater tensile strength than composites reinforced with sisal fibers.

- Tensile strength of N-FRP composites hybridized with Jute and Sisal fibers is 44.9% higher than that of Sisal fibre reinforced composites.
- The unique characteristics of each fibre are combined by the hybridization process to create a composite material with improved mechanical properties and a higher resistance to fracture and cracking under tension.
- Holes are successfully machined on hybrid N-FRP using the R-ECDM technique with different tool rotation and electrolyte concentrations.
- Increases in electrolyte concentration from 15 wt.% to 20 wt.% and in tool rotation from 355 rpm to 900 rpm are observed to cause increases in surface roughness of 15.8% and 33%, respectively.
- By preventing sparks from originating at a single point, tool rotation greatly improves hole geometry and produces more uniform spark dispersion.
- An improvement of 36.3 % and 29.8 % in HOC and CE is computed with the application of tool rotational effect in ECDM compared to conventional ECDM process.
- When tool rotation is used, the surface roughness of holes is greatly reduced when compared to conventional ECDM process owing to prevention of side and stray sparking.

### Acknowledgement

Authors are thankful to the Punjab Engineering College, Chandigarh for their support.

### REFERENCES

1. Ku H, Wang H, Pattarachaiyakop N, Trada M. A review on the tensile properties of natural fiber reinforced polymer composites. *Composites Part B: Engineering*. 2011 Jun 1;42(4):856-73.
2. Reddy N, Yang Y. Potential of plant proteins for medical applications. *Trends in biotechnology*. 2011 Oct 1;29(10):490-8.
3. Gholampour A, Ozbakkaloglu T. A review of natural fiber composites: Properties, modification and processing techniques, characterization, applications. *Journal of Materials Science*. 2020 Jan;55(3):829-92.
4. Binder WH. The past 40 years of macromolecular sciences: reflections on challenges in synthetic polymer and material science. *Macromolecular Rapid Communications*. 2019 Jan;40(1):1800610.
5. Elfaleh I, Abbassi F, Habibi M, Ahmad F, Guedri M, Nasri M, Garnier C. A comprehensive review of natural fibers and their composites: an eco-friendly alternative to conventional materials. *Results in Engineering*. 2023 Jul 1:101271.
6. Singh MK, Tewari R, Zafar S, Rangappa SM, Siengchin S. A comprehensive review of various factors for application feasibility of natural fiber-reinforced polymer composites. *Results in Materials*. 2023 Mar 1;17:100355.
7. Sonali S, Farzana M, Haque MM, Saha A, Khan RA, Mollah MZ. Natural fiber reinforced polymer-based composites: importance of jute fiber. *GSC Advanced Research and Reviews*. 2023;15(1):021-9.
8. Tajuddin M, Ahmad Z and Ismail H. A review of natural fibers and processing operations for the production of binderless boards. *BioResources*, 2016, 11(2): 5600-5617.
9. Abilash N and Sivapragash M. Environmental benefits of eco-friendly natural fiber reinforced polymeric composite materials. *International Journal of application or innovation in Engineering and management (IJAIEEM)*, 2013, 2(1): 53-59.
10. Mohammed L, Ansari MN, Pua G, Jawaid M, Islam MS. A review on natural fiber reinforced polymer composite and its applications. *International journal of polymer science*. 2015 Oct 1;2015.
11. E. Jayamani, S. Hamdan, M. R. Rahman, and M. K. B. Bakri, "Comparative study of dielectric properties of hybrid natural fiber composites," *Procedia Engineering*, vol. 97, pp. 536–544, 2014.
12. C. C. Eng, N. A. Ibrahim, N. Zainuddin, H. Ariffin, and W. M. Z. W. Yunus, "Impact strength and flexural properties enhancement of methacrylate silane treated oil palm mesocarp fiber reinforced biodegradable hybrid composites," *The ScientificWorld Journal*, vol. 2014, Article ID 213180, 8 pages, 2014.

13. K. Bocz, B. Szolnoki, A. Marosi, T. T´abi, M. Wladyka-Przybylak, and G. Marosi, “Flax fibre reinforced PLA/TPS biocomposites flame retarded with multifunctional additive system,” *Polymer Degradation and Stability*, vol. 106, pp. 63–73, 2014.
14. O. Faruk, A. K. Bledzki, H.-P. Fink, and M. Sain, “Biocomposites reinforced with natural fibers: 2000–2010,” *Progress in Polymer Science*, vol. 37, no. 11, pp. 1552–1596, 2012.
15. Rubio-López A, Artero-Guerrero J, Pernas-Sánchez J, Santiuste C. Compression after impact of flax/PLA biodegradable composites. *Polymer Testing*. 2017 May 1; 59:127-35.
16. Keck S, Fulland M. Effect of fibre volume fraction and fibre direction on crack paths in flax fibre-reinforced composites. *Engineering Fracture Mechanics*. 2016 Nov 1; 167:201-9.
17. Okubo K, Fujii T and Yamamoto Y. Development of bamboo-based polymer composites and their mechanical properties. *Composites Part A: Applied Science and Manufacturing*, 2004, 35(3): 377-383.
18. Jiang L, Huang J, Qian J, Chen F, Zhang J, Wolcott MP, Zhu Y. Study of poly (3-hydroxybutyrate-co-3-hydroxyvalerate) (PHBV)/bamboo pulp fiber composites: Effects of nucleation agent and compatibilizer. *Journal of Polymers and the Environment*. 2008 Apr; 16:83-93.
19. Nino Serah Baby, N. Sakthieswaran, G. Shiny Brintha & O. Ganesh Babu, “A Review on Hybrid Composites Reinforced with Sisal Fibers, Glass Fibers, Steel Fibers and Prosopis Juliflora”, *International Journal for Research in Applied Science and Engineering Technology*, May 2016, Volume 4 Issue V, ISSN: 2321-9653.
20. Karina M, Onggo H, Syampurwadi A. Physical and mechanical properties of natural fibers filled polypropylene composites and its recycle. *Journal of Biological Sciences*. 2007;7(2):393-6.
21. Rajput V, Goud M, Suri NM. Performance analysis of ECDM process using surfactant mixed electrolyte. In *Manufacturing Engineering: Select Proceedings of CPIE 2019*; (pp. 285-300). Springer Singapore.
22. Rajput V, Pundir SS, Goud M, Suri NM. Multi-response optimization of ECDM parameters for silica (quartz) using grey relational analysis. *Silicon*. 2021 May; 13:1619-40.
23. H. Kurafuji, K. Suda, Electrical discharge drilling of glass, *CIRP Ann.*, 16, 415-419, 1965.
24. Basak I, Ghosh A. Mechanism of spark generation during electrochemical discharge machining: a theoretical model and experimental verification. *Journal of Materials Processing Technology*. 1996 Nov 1;62(1-3):46-53.
25. Basak I, Ghosh A. Mechanism of material removal in electrochemical discharge machining: a theoretical model and experimental verification. *Journal of materials processing technology*. 1997 Nov 23;71(3):350-9.
26. Zheng ZP, Cheng WH, Huang FY, Yan BH. 3D microstructuring of Pyrex glass using the electrochemical discharge machining process. *Journal of micromechanics and microengineering*. 2007 Apr 12;17(5):960.
27. Malik A, Manna A. An experimental investigation on developed WECSM during micro slicing of e-glass fibre epoxy composite. *The International Journal of Advanced Manufacturing Technology*. 2016 Aug; 85:2097-106.
28. Rajput V, Goud M, Suri NM. Performance analysis of ECDM process using surfactant mixed electrolyte. In *Manufacturing Engineering: Select Proceedings of CPIE 2019 2020* (pp. 285-300). Springer Singapore.
29. Gautam N, Jain VK. Experimental investigations into ECSD process using various tool kinematics. *International Journal of Machine Tools and Manufacture*. 1998 Jan 1;38(1-2):15-27.
30. Rajput V, Goud M, Suri NM. Enhancement of Electrochemical Discharge Machining (ECDM) Characteristics with Tool Electrode Rotation. In *Advances in Modelling and Optimization of Manufacturing and Industrial Systems: Select Proceedings of CIMS 2021 2023 Feb 24* (pp. 135-148). Singapore: Springer Nature Singapore.
31. Rajput V, Goud M, Suri NM. Performance analysis of closed-loop electrochemical discharge machining (CLECDM) during micro-drilling and response surface methodology based multi-response parametric optimisation. *Advances in materials and processing technologies*. 2022 Apr 3;8(2):1352-82.

32. Singh M, Singh S. Micro-machining and process optimization of electrochemical discharge machining (ECDM) process by TOPSIS method. In *Advances in Manufacturing II: Volume 2- Production Engineering and Management 2019* (pp. 206-215). Springer International Publishing.
33. Garg MP, Singh M, Singh S. Micro-machining and process optimization of electrochemical discharge machining (ECDM) process by GRA method. In *Advances in Manufacturing II: Volume 4-Mechanical Engineering 2019* (pp. 384-392). Springer International Publishing.
34. Rajput V, Goud M, Suri NM. Electrochemical discharge machining: gas film electrochemical aspects, stability parameters, and research work. *Journal of the electrochemical society*. 2021 Jan 13;168(1):013503.
35. Huang SF, Liu Y, Li J, Hu HX, Sun LY. Electrochemical discharge machining micro-hole in stainless steel with tool electrode high-speed rotating. *Materials and Manufacturing Processes*. 2014 May 4;29(5):634-7.
36. Bhargav KV, Balaji PS, Sahu RK, Katiyar JK. Exemplary approach using tool rotation-assisted  $\mu$ -ECDM for CFRP composites machining. *Materials and Manufacturing Processes*. 2023 Feb 17;38(3):271-83.
37. Rajput V, Bhinder J, Singh G. Research Progress of Self-Healing Elastomers Materials: Processing and Characterization. *Materials for Biomedical Simulation: Design, Development and Characterization*. 2023 Sep 27:59-69.
38. Rajput V, Nagori I, Goud M, Suri NM, Chaudhary GR, Bhinder J. Development and Analysis of Polymer-Based Self-Healing Composite Embedded with Silica (SiO<sub>2</sub>) Hollow Glass Fibers. *Silicon*. 2023 Nov;15(17):7279-92.
39. Ranganayakulu J, Srihari PV, Rao KV, Raj RS, Mahajanshetti M. Machining Strategies for Micromachining of Glass Using Electrochemical Discharge Machining: A Review. *Innovative Development in Micromanufacturing Processes*. 2024:132-53.
40. MALLICK B, DOLOI B, SARKAR B, BHATTACHARYYA B. MICRO-MACHINING PERFORMANCES BY ECDM PROCESS FOR NON-CONDUCTING MATERIALS. *Electro-Micromachining and Microfabrication: Principles and Research Advances*. 2024 Apr 9:71.
41. Sivakandhan C, Murali G, Tamiloli N, Ravikumar L. Studies on mechanical properties of sisal and jute fiber hybrid sandwich composite. *Materials Today: Proceedings*. 2020 Jan 1;21:404-7.